Numerical and experimental investigation of geothermal integration into tunnels

Recherches numériques et expérimentales sur l'intégration géothermique dans les tunnels

Asal Bidarmaghz, Guillermo A. Narsilio,
Department of Infrastructure Engineering, The University of Melbourne, Australia narsilio@unimelb.edu.au

Patrik Buhmann, Christian Moormann, Bernhard Westrich
Institute of Geotechnical Engineering, University of Stuttgart, Germany

ABSTRACT: Renewable geothermal energy can be harvested through Ground Heat Exchangers (GHEs) using almost any engineering structure that is in contact with the ground, such as tunnels. The integration of geothermal loops into tunnels leads to a substantially large ground volume made available for geothermal exchange. The aim of this paper is to model and evaluate the integration of geothermal loops into tunnels to heat and cool targeted spaces and to provide insights into the heat transfer mechanisms and potential thermal interactions with existing nearby GHEs. A new 3D model is developed and solved numerically to simulate the thermo-hydro processes in the ground and the geothermal tunnel lining using the finite element package COMSOL Multiphysics. Numerical results are then validated against measured data from the Fasanenhof Tunnel (Stuttgart, Germany), where two sections of the tunnel have been equipped with geothermal loops. The efficiency of the system is investigated under selected possible scenarios. Numerical results together with full-scale measured data indicate that geothermal tunnels shows potential to exploit the available geothermal energy in the ground allowing heating and cooling spaces such as nearby buildings and stations.

RÉSUMÉ: Ces renouvelable énergie géothermique peut être récoltée par échangeurs de chaleur au sol (GHEs) en utilisant presque n'importe quelle structure d'ingénierie en contact avec le sol, comme les tunnels. Le but de cet article est de modéliser et d'évaluer l'intégration de boucles géothermiques dans des tunnels pour chauffer et refroidir des espaces ciblés et pour donner un aperçu des mécanismes de transfert de chaleur et des interactions thermiques potentielles avec les GHE voisins. Un nouveau modèle 3D est développé et résolu numériquement pour simuler les processus thermo-hydro dans le sol et le revêtement de tunnel géothermique en utilisant le paquet d'éléments finis COMSOL Multiphysics. Les résultats numériques sont ensuite validés à partir des données mesurées du tunnel Fasanenhof (Stuttgart, Allemagne), où deux tronçons du tunnel ont été équipés de boucles géothermiques. L'efficacité du système est étudiée sous différents scénarios possibles d'écoulement des eaux souterraines. Les résultats numériques ainsi que les données mesurées à pleine échelle indiquent que les tunnels géothermiques montrent un potentiel d'exploitation de l'énergie géothermique disponible dans le sol permettant des espaces de chauffage et de refroidissement tels que des bâtiments et des stations à proximité.

KEYWORDS: energy tunnels, finite elements, geothermal, full scale testing

1 INTRODUCTION

Shallow geothermal energy systems extract and reject heat from and to the ground within a few tens to hundreds of metres below the surface with the help of a Ground Source Heat Pump (GSHP). GSHP systems provide efficient space heating and cooling. These systems are known to typically be able to run at a coefficient of performance of about four, delivering approximately 4 kW of heating/cooling energy for every 1 kW electricity input into the heat pump (Preene & Powrie 2009; Johnston et al. 2011; Lund & Boyd 2015). A GSHP connects a heating and cooling distribution circuit within a building with a series of ground heat exchangers (GHEs). A GHE typically consists of a structure with embedded high density polyethylene (HDPE) loops in which a carrier fluid (usually water) circulates.

The thermal activation of geostructures such as piles or diaphragm walls has recently become more widespread (Adam and Markiewicz, 2009, Unterberger et al., 2004). This dual purpose (structural and thermal) can be also extended to tunnel linings, converting them into GHEs owing to their high degree of contact with the subsoil.

Geothermal loops embedded into tunnel lining exchange heat with the surrounding ground and with the air inside the tunnel. The exchange of heat arising from the tunnel GHEs may interfere with existing vertical borehole ground heat exchangers (BHEs) adjacent to the tunnel.

In all cases, the heat extraction rate is influenced by the thermal properties of the ground, farfield ground temperature, the presence of groundwater (and groundwater movement), the geometrical arrangement of the absorber HDPE pipes and spacing between heat exchangers (e.g., tunnels, BHEs).

This paper investigates the thermal interaction between the geothermally activated tunnels (tunnel GHEs) and adjacent BHEs and how the operation of either might affect the thermal performance of the other as well as the role of groundwater flow in this thermal interaction.

To simulate heat transfer in energy tunnels, BHEs and the surrounding ground, a calibrated, validated 3D numerical model based on fundamental principles has been implemented using finite element methods. The governing equations for fluid flow and heat transfer are coupled numerically within the finite element package COMSOL Multiphysics. Heat transfer in the ground is modelled by both conduction and convection due to the groundwater movement. Pure conduction occurs in the HDPE pipe wall, grouted BHE, tunnel lining and partially in the carrier fluid (water). Heat convection dominates in the carrier fluid circulating in the absorber pipes.

This model is validated against experimental data from the Stuttgart-Fasanenhof tunnel, Germany, for which two tunnel blocks, 10 m each are geothermally activated and equipped with sophisticated measurement transducers for research purposes (Moormann et al., 2015).

2 FINITE ELEMENT MODEL

The hydro-thermal responses of the porous ground, tunnel GHEs, the vertical BHE and the ground water are numerically coupled and solved using finite element methods.

2.1 *Geometry*

To study the thermal interaction between BHEs and geothermal tunnels, a 10m diameter tunnel with a simplified circular section (0.4 m of lining thickness) 10 m below the ground surface is modelled together with a 30 m deep single U-loop, 125 mm diameter BHE, located at 3 m horizontal distance from the tunnel. The selection of a short BHE (30 m long) is made to maximise these thermal interactions. Ground water flow is considered in this study. The BHE U-pipe separation is 0.08 m. HDPE pipes in both the BHE and the tunnel GHEs are of 0.025 m outer diameter (SDR 11). Two circuits of about 200 m HDPE pipes are embedded in every 10 m longitudinal section of the tunnel (x-axis). For simplicity, only a 10 m wide section of the tunnel and the surrounding ground is considered in the simulations (zy planes of symmetry considered, Figure 1).

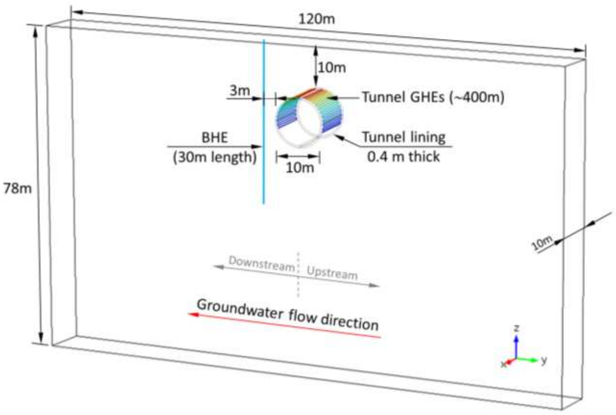

Figure 1 Tunnel and borehole heat exchanger Schematics

2.2 *Governing Equations: Brief Description*

The governing equations for fluid flow and heat transfer (conduction, convection and radiation) are coupled numerically within the finite element package COMSOL Multiphysics to evaluate the thermal performance of the BHE and the tunnel GHEs. Details can be found in Narsilio et al. 2016.

Heat conduction occurs in the ground (porous material), in the BHE backfilling material (concrete), the tunnel lining and in the absorber pipe wall (both in tunnels GHEs and the BHE), and partially in the carrier fluid (water) circulating within the tunnel GHEs and the BHE. Heat convection dominates in the carrier fluid circulating in the pipes (in tunnel GHEs and the BHE) and in the ground due to the groundwater movement.

To model the fluid flow inside the HDPE pipes, the continuity and momentum equations for incompressible fluid are used.

$$\nabla.(A\rho_w \mathbf{v_1}) = 0 \tag{1}$$

$$\rho_w\left(\frac{\partial \mathbf{v_1}}{\partial t}\right) = -\nabla p_1 - f_D\frac{\rho_w}{2d_h}|\mathbf{v_1}|\mathbf{v_1} \tag{2}$$

These equations are coupled to an energy equation for the fluid flow to describe the convective-conductive heat transfer in the pipes for an incompressible (Lurie, 2008):

$$\rho_w A C_{p,w}\frac{\partial T}{\partial t} + \rho_w A C_{p,w}\mathbf{v_1}\nabla T = \nabla(A\lambda_w\nabla T) + f_D\frac{\rho_w A}{2d_h}|\mathbf{v_1}|\mathbf{v_1}^2 + Q_{wall}$$

$$Q_{wall} = f(T_{(m,pipe\ wall)}, T) \tag{3, 4}$$

where A is the inner cross-section of the HDPE pipe, ρ_w is the carrier fluid density, $\mathbf{v_1}$ represents the fluid velocity field in the pipes embedded within the tunnel GHEs and BHEs, t is time, p_1 is pressure, f_D represents the Darcy friction factor, d_h is the hydraulic diameter of the pipe, $C_{p,w}$ is the specific heat capacity of the fluid, λ_w is thermal conductivity of the fluid and Q_{wall} is the external heat exchange rate through the pipe wall and it is a function of the temperature of the pipe outer wall, $T_{(m,pipe,\ wall)}$ and the temperature of the carrier fluid, T (Bidarmaghz and Narsilio, 2016, Narsilio et al., 2016). The above equations are solved for pressure p_1, velocity field $\mathbf{v_1}$ and temperature field T in the carrier fluid and are coupled to the ground temperature field T_m obtained from the conductive-convective heat transfer equations solved for the BHEs filling material, tunnel lining, the pipe walls and surrounding permeating ground (Eq. 3). It should be noted that in BHEs, absorber pipe wall and tunnel lining, heat transfer process is purely conductive

$$(\rho C_p)_{eff}\frac{\partial T_m}{\partial t} + (\rho C_p \mathbf{v_2})\nabla T_m + \nabla.\lambda_{eff}\nabla T_m = 0 \tag{5}$$

The groundwater flow is described by Darcy's law, where the Darcy velocity field, $\mathbf{v_2}$ is determined by the total head gradient $\nabla(p_2 - \rho_f \mathbf{g}\, z)$ and groundwater dynamic viscosity, μ_f,:

$$\boldsymbol{v_2} = -K/\mu_f\,\nabla(p_2 - \rho_f g z) \tag{6}$$

$$\nabla.(\rho_f \boldsymbol{v_2}) = 0 \tag{7}$$

where K is the isotropic intrinsic permeability of the ground, p_2 is pore pressure, ρ_f is the groundwater density, and $\mathbf{g}$ is the gravitational acceleration vector.

Figure 2 shows the initial and boundary conditions prescribed here to solve the above systems of equations. Table 1 summarises key input material parameters used.

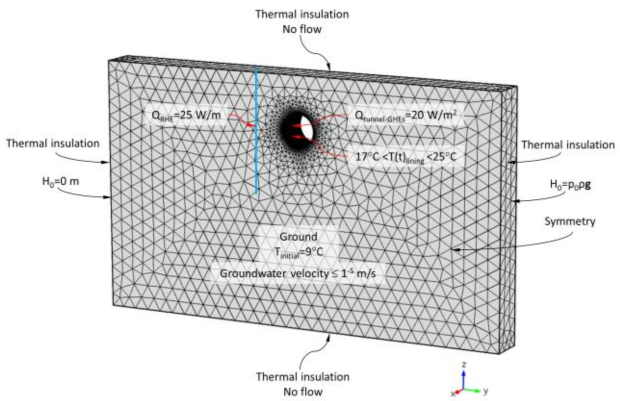

Figure 2 Boundary conditions

Table 1. Key input parameters used in the numerical models.

Material	λ W/(mK)	C_p J/(kgK)	ρ kg/m^3
Ground	2.0	1,100	2,400
Concrete	2.1	890	2,250
HDPE (pipe)	0.4	-	-
Carrier fluid	0.582	4,180	1,000

2.3 *Model Validation*

The 3D numerical model developed for the simulation of the thermal interaction between the tunnel GHEs and BHEs is first validated against measured thermal data from a full-scale testing and monitoring geothermal tunnel (Fasanenhof tunnel, Stuttgart, Germany) subjected to 6 months of cooling (04/2012 to 10/2012) (Moormann et al., 2015).

Details of the initial and boundary conditions are shown in Figure 3-a. The geometry of this model is analogous to Figure 1. However, no BHE exists in the vicinity of the tunnel.

The numerical model simulates the aforementioned 6 months of cooling through the GHEs embedded in the tunnel lining (25 mm pipe outer diameter, SDR 11 with T_{inlet}=20.9°C, 560 L/hr (0.47 m/s) <q< 1085 L/hr (0.92 m/s)). The key input parameters used in the validation were listed in Table 1.

Figure 3-bottom shows the good agreement between the average fluid temperature in the tunnel GHE ($T_{average}=(T_{in}+T_{out})/2$) obtained numerically and measured experimentally (T_{in} located laterally on both sides of the tunnel, T_{out} located at the tunnel apex). This good agreement brings confidence on the ability of the model about capturing well the main physical processes involved.

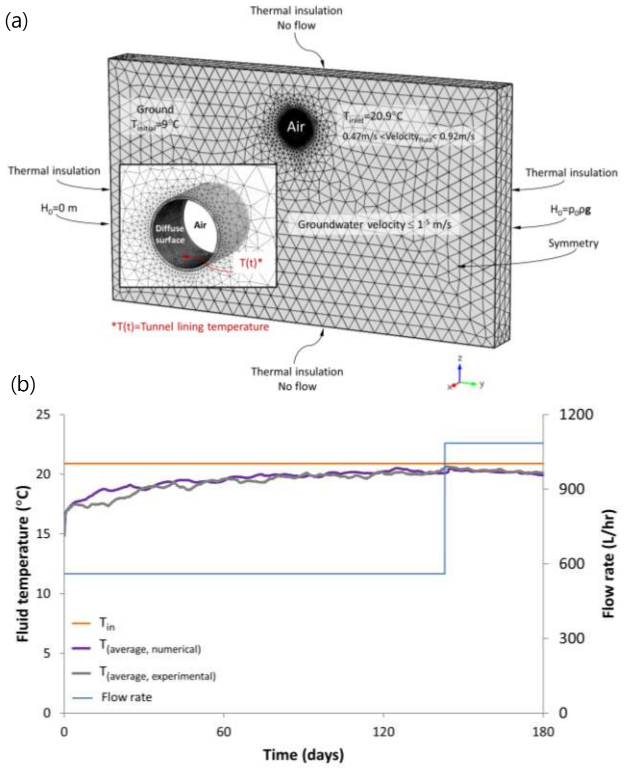

Figure 3. Validation model: initial and boundary conditions (a), and comparison of numerical and experimental results (b)

4. INTERACTION BETWEEN TUNNEL GHES AND BHES

To investigate the potential thermal interaction between the tunnel and adjacent BHEs with 25 W/m extraction and rejection (depending on season), selected scenarios are solved using transient 3D simulations. The analysed cases are summarised in Table 2. The geometry of the models was previously shown in Figure 1 together with initial and boundary conditions in Figure 2. The presence of groundwater flow perpendicular to the main axis of the tunnel results in a non-symmetrical temperature distribution around the tunnel. Thus, the thermal interaction between tunnel and BHE is investigated for BHEs located upstream and downstream of the tunnel. Results are compared to a BHE only scenario (case 3) where no geothermal tunnel exists in the vicinity of the BHE.

The average annual maximum and minimum BHE wall temperature for the first 5 years of operation are shown in Figure 4 for cases 1, 2, 3 and 4. One can see that the BHE wall temperature for BHEs located downstream (case 1) is about 2 to 2.5°C higher within 5 years than the other two scenarios (cases 2 and 3), which is beneficial to the ground source heat pump (GSHP) systems using those downstream BHEs given the heating dominant nature of the thermal demand defined for all these cases. The heat generated inside the tunnel (as a result of heat rejection from metro trains to the tunnel air, e.g., train breaks) is used up by the tunnel GHEs and the excess heat moves by convection towards the downstream BHE due to the groundwater movement resulting in higher temperatures within the downstream BHE walls. Comparing the BHE wall temperatures for case 1 (BHE and geothermal tunnel model) and case 3 (BHE only model) indicates that the thermal interaction between the tunnels and the BHEs improves the thermal performance of BHE (in heating dominant conditions) as it shows significantly higher average BHE temperature in comparison to a standalone BHE.

Table 2. Scenarios investigated in this work

Case	Tunnel GHEs	BHE	G.W. flow	BHE Position
1	✓	✓	✓	Downstream
2	✓	✓	✓	Upstream
3	×	✓	✓	-
4	✓	✓	×	Downstream

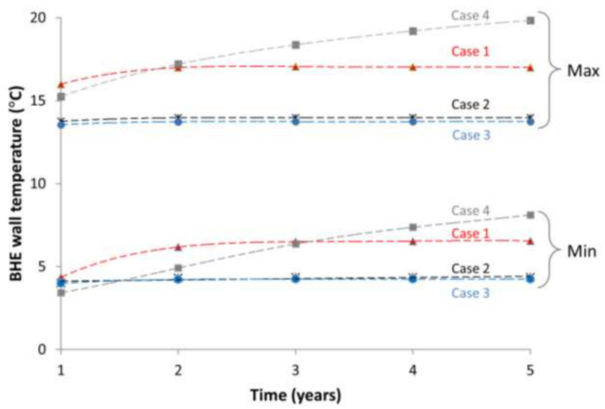

Figure 4 Average BHE wall temperature for different scenarios

On the other hand, comparing identical cases where groundwater flow is considered or not (cases 1 and 4) shows that groundwater flow makes the BHE to reach steady-state temperature faster due to the prevention of heat accumulation around the borehole, as depicted in Figure 5.

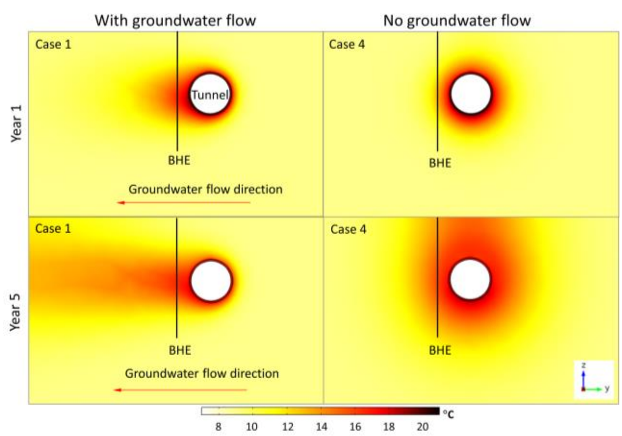

Figure 5. Temperature distribution around the BHEs and the tunnel for cases 1 and 4.

Figure 6 shows the ground temperature at mid-depth of the BHE and tunnel centre (15 m below the ground surface) along 60 m (in the y-direction) for two scenarios: a BHE in the vicinity of metro tunnel (case 1) and a standalone BHE (case 3) at the end of the heating season (top) and at end of the cooling season (b) after 5 years of operation.

An operational geothermal tunnel and BHE (case 1) at the end of the heating season (Figure 6-top) shows significantly higher ground temperature in the tunnel and BHE vicinity in comparison to a standalone BHE (case 3). This temperature difference is due to the convective heat transfer driven by groundwater flow from the tunnel to the BHE. The ground temperature around the tunnel and the BHE is between 4°C (at a point 30 m downstream) and 11°C (at the tunnel wall) higher in case 1 than in case 3. This figure suggests that the presence of 'hot' tunnels in heating dominant climate conditions tend to improve the thermal performance of nearby downstream BHE since the heat generated inside the tunnels will be transported through the groundwater flow direction toward the downstream BHE. The significantly lower temperature reached within the BHE (mid-depth) for case 3 (9.4°C) vs. case 1 (12.7°C) during the heating season also highlights the importance of thermal interaction between the tunnel and the BHE.

Similarly, Figure 6-b shows the ground temperature at the end of 3 months of cooling. The results indicate that the thermal interaction between the BHE and the 'hot' tunnels are detrimental to the thermal performance of downstream BHE in cooling seasons given that it results in about 4°C higher temperatures reached within the BHE (18.1◦C in case 1 vs. 14.1°C in case 3). Moreover, the ground temperature around the tunnel and BHEs is between 9°C (at a point 30 m downstream) and 17°C (at the tunnel wall) higher in the BHE and tunnel scenario (case 1) than in the BHE only scenario (case 3). the proposed relationship in Equation 2 is best represented.

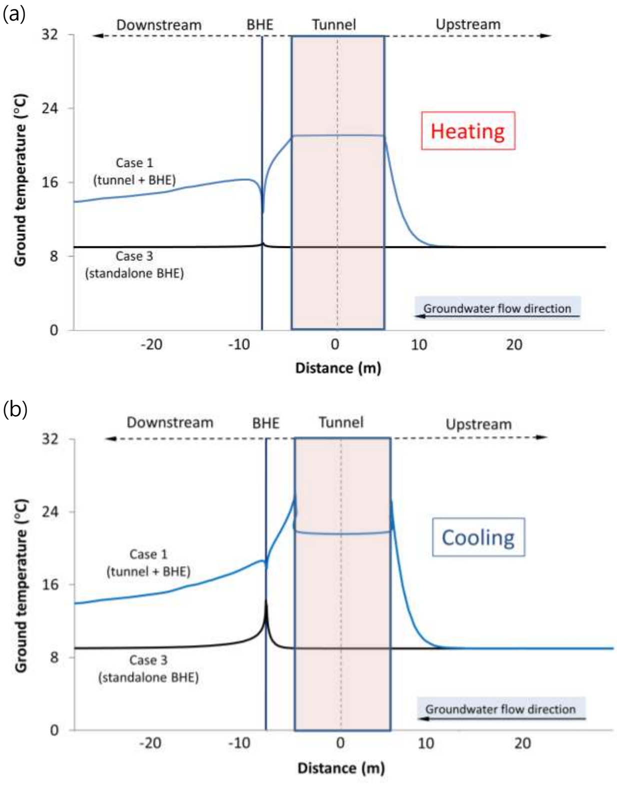

Figure 6. Comparison of ground temperature around the BHE and the tunnel at the end of heating season (a), and at the end of the cooling season (b)

4 CONCLUSION

This study is based on the development of a detailed 3D finite element model used to investigate the effects of thermal interaction between geothermal tunnels and adjacent BHEs under few selected conditions. First insights into the thermal performance of BHEs affected by such interactions have been presented.

The numerical results show that vertical BHEs in the vicinity of geothermal tunnels may benefit from the heat generated inside the metro 'hot' tunnels and also from the tunnel GHEs operation. This heat transferred to the surrounding ground through groundwater flow, affecting only BHEs located downstream. BHEs located upstream show similar results to standalone BHEs, even in the presence of groundwater flow.

In the absence of groundwater flow, the BHE generally experiences a higher average temperature throughout the year, which may be more beneficial in places with heating dominant demand. The ground temperature fields obtained from the numerical simulations indicate that in general, BHEs close to geothermal perform significantly better in comparison to far away BHEs as they show significantly higher average temperature (heating dominant climate conditions), which is at highest when there is no groundwater flow in the ground. However, this statement is valid for BHEs close enough to the tunnels. It is expected that for BHEs further away from the tunnels, the groundwater flow improves the thermal performance of BHEs, but to a varying lesser degree. Importantly, the addition of GHEs to tunnel linings does not seem to significantly impact on the performance of BHEs in the proximity of the tunnels and the conditions analysed here. Future work includes assessing the influences of groundwater velocity and the ratio of distance between geothermal tunnels and BHEs to tunnel diameter.

5 ACKNOWLEDGEMENTS

Funding from the Australian Research Council (ARC) FT140100227, The University of Melbourne and the Victorian Government is much appreciated.

6 REFERENCES

Adam, D. & Markiewicz, R. (2009) Energy from earth-coupled structures, foundations, tunnels and sewers. *Géotechnique* 59(3):229-236.

Bidarmaghz, A. & Narsilio, G. (2016) Shallow geothermal energy: emerging convective phenomena in permeable saturated soils. *Géotechnique Letters* 6(2):119-125.

Johnston, I., Narsilio, G., and Colls, S. (2011). Emerging geothermal energy technologies.*KSCE J of Civil Eng*, 15(4), 643-653.

Lund, J. and Boyd, T. 2015. Direct utilization of geothermal energy 2015 worldwide review. *Proceedings World Geothermal Congress,* April 2015. pp. 25-29.

Lurie, M. V. (2008) *Modeling and Calculation of Stationary Operating Regimes of Oil and Gas Pipelines.* Weinheim, Germany, Wiley-VCH Verlag GmbH & Co. KGaA.

Moormann, C., Buhmann, P., Pralle, N. & Friedemann, W. (2015) International experience on regenerative energy concepts in tunnel projects. In *International symposium on energy geotechnics (SEG).*) ISSMGE TC308, Paris, France.

Narsilio, G. A., Bidarmaghz, A., Johnston, I. W. & Colls, S. (2016) Detailed numerical modelling of ground heat exchangers based on first principles. *Computers & Geotechnique* (under review).

Preene, M., and Powrie, W. (2009). "Ground energy systems: from analysis to geotechnical design." Géotechnique, 59(3), 261-271.

Unterberger, W., Hofinger, H., Grünstäudl, T., Adam, D. & Markiewicz, R. (2004) Utilization of tunnels as sources of ground heat and cooling–Practical applications in Austria. In *Proceedings of the ISRM International Symposium 3rd ARMS, Kyoto*.), pp. 421-426.